TECHNICAL NOTES

NATIONAL ADVISORY COMMITTEE FOR AERONAUTICS

No. 386

EFFECT OF NOSE SHAPE ON THE CHARACTERISTICS OF SYMMETRICAL AIRFOILS

By Robert M. Pinkerton
Langley Memorial Aeronautical Laboratory

Washington
August, 1931

NATIONAL ADVISORY COMMITTEE FOR AERONAUTICS

TECHNICAL NOTE NO. 386

EFFECT OF NOSE SHAPE ON THE CHARACTERISTICS OF SYMMETRICAL AIRFOILS

By Robert M. Pinkerton

Summary

Tests of nine symmetrical airfoils, having different leading-edge radii, were made in the variable density wind tunnel. Three symmetrical N.A.C.A. airfoils having maximum thickness-to-chord ratios of 0.06, 0.12, and 0.18 were used as basic (or normal) sections; and for each of these thicknesses one thinner and one blunter nose section were developed. The thin-nosed sections gave lower minimum drags and lower maximum lifts than the normal sections. The blunt-nosed sections gave higher minimum drags and higher maximum lifts than the normal sections except for the thickest section which showed a lower maximum lift. The rate of increase of drag with lift is greater for the thin-nosed sections. Finally, although the slope of the lift curve varies with thickness, these tests show that for any given thickness the slope is independent of nose radius.

Introduction

A comprehensive investigation of the relation between the geometric and aerodynamic characteristics of airfoils at a high value of the Reynolds Number is in progress in the variable density wind tunnel of the National Advisory Committee for Aeronautics. (Reference 1.) The principal variables are those of thickness and camber, but it was thought advisable to include also a study of the effect of changes in nose radius.

This report presents the results of tests of nine symmetrical airfoils having different leading-edge radii. Three of the symmetrical N.A.C.A. airfoils, designated N.A.C.A. 0006, N.A.C.A. 0012, and N.A.C.A. 0018, having

maximum thickness-to-chord ratios of 0.06, 0.12, and 0.18, respectively, were chosen as the basic (or normal sections), and for each of these one thinner and one blunter nose section were developed and tested. The derivation of each modified section was accomplished by a systematic change in the equation that defines the normal section. This change is principally a change in nose radius, but it also results in modifications to the profile throughout its length, except at the maximum ordinate and at the trailing edge.

Description of Airfoils

The method of deriving the normal sections is discussed in reference 1. In brief, they are defined by an equation of the form

$$y = a_0\sqrt{x} + a_1x + a_2x^2 + a_3x^3 + a_4x^4 \qquad (1)$$

from which it is found that the nose radius is given by

$$r = \frac{a_0^2}{2} \qquad (2)$$

The conditions used to evaluate the above constants are as follows:

Maximum ordinate:	$x = 0.3$	$y = 0.1$
		$\frac{dy}{dx} = 0$
Trailing-edge thickness:	$x = 1$	$y = 0.002$
Trailing-edge angle:	$x = 1$	$\frac{dy}{dx} = -0.234$
Nose shape:	$x = 0.1$	$y = 0.078$

From the resulting equation

$$y = 0.2969\sqrt{x} - 0.1260x - 0.3516x^2 + 0.2843x^3 - 0.1015x^4$$

the ordinates have been calculated and are given in Table I.

The thin-nosed sections are derived in a similar manner and are denoted by the suffix T. The constants are determined for the same conditions as above except for the nose-shape condition, which is

$$r_T = 1/4\ r$$

where r_T is the nose radius of the thin-nosed section. By means of equation (2)

$$a_{o_T} = 1/2\ a_o = 0.1484$$

where a_{o_T} is the value of a_o for the thin-nosed section, and finally

$$y_T = 0.1484\sqrt{x} + 0.3493x - 1.2890x^2 + 1.2520x^3 - 0.4588x^4$$

Ordinates calculated from this equation are given in Table I.

The blunt-nosed sections, similarly derived, are denoted by the suffix B. For this group

$$r_B = 3\ r$$

hence

$$a_{o_B} = \sqrt{3}\ a_o = 0.5144$$

and

$$y_B = 0.5144\sqrt{x} - 0.8180x + 1.0140x^2 - 1.1328x^3 + 0.4245x^4$$

Table I contains ordinates calculated from this equation.

The ordinates for the sections used in this investigation were obtained by multiplying the ordinates given in Table I by the factor $\frac{t}{0.20}$ where t is the desired value of the maximum thickness-to-chord ratio. When the thick profiles of the blunt-nosed series were plotted, the nose appeared so extremely blunt that it seemed desirable to reduce the nose radii of the 0012B and 0018B. This reduction was accomplished graphically and the results are

given in Table II. Because of this arbitrary reduction of nose radii it was found necessary to modify the calculated ordinates of the 0018B at the stations x = 1.25 per cent and 2.50 per cent of the chord.

Because each of these modified sections was defined by an equation to produce fairness, some differences, of course, have appeared throughout the profile as a result of the change in nose radius. These differences (fig. 1) are small, however, as compared to the differences at the nose; hence the nose radius is considered as the independent variable.

The models were made of duralumin and have a chord of 5 inches and a span of 30 inches. The method of construction is described in reference 1.

Tests and Results

Routine measurements of lift, moment, and drag were made in the variable density wind tunnel at a tank pressure of about 20 atmospheres. The Reynolds Number of the tests is about 3,000,000. A detailed description of the tunnel and the test procedure is given in reference 1.

The results of these tests are presented in the form of coefficients corrected, after the method of reference 2, to give infinite aspect ratio characteristics. Values of the lift coefficient C_L, angle of attack for infinite aspect ratio α_o, profile drag coefficient C_{D_o}, and moment coefficient $C_{m_{c/4}}$ are given in Tables III to XI. Figures 2 to 4 present the usual lift-curve plots and Figure 5 shows the variation of maximum lift coefficient and minimum profile drag coefficient with nose radius. Plots of moment coefficient against lift coefficient are given in Figure 6. Profile drag curve plots are given in Figures 7 to 9.

Discussion

Changes in the lift characteristics accompanying changes in the nose radius may be observed in Figures 2 to

5. Although the slope of the lift curve varies with thickness, Figures 2 to 4 show that for any given thickness the slope is independent of nose radius. The dotted portions of some of the curves indicate an unstable condition which in some instances amounts to a sharp discontinuity in the lift forces as shown by a sudden drop of the lift balance beam. These tests show that the discontinuities disappear in the thin-nosed sections. As shown by Figure 5, the maximum lift decreases in every instance when the nose radius of the normal section is decreased and increases, for the 0006 and 0012, when the nose radius of the normal section is increased. Increasing the nose radius of the normal 0018 resulted in a decreased maximum lift.

The variation of pitching moment with lift is shown in Figure 6. Increasing the nose radius leads to an increase of the slope of the curve of $C_{m_{c/4}}$ against C_L; that is, the position of the center of pressure is farther forward for the blunter section. The position of the center of pressure at $C_L = 0.4$ for the 0018B, which shows the greatest slope, is $22\frac{1}{2}$ per cent of the chord behind the leading edge. In passing, it must be noted that the 0006T and 0006B moment data are obviously in error since a symmetrical section can have no moment at zero lift. No explanation could be found for this apparent shift of the pitching moment, although the models were checked for symmetry. However, this shift is small and would not be expected to affect the other measurements.

The effect of nose shape on the variation of profile drag with lift is shown in Figures 7 to 9. Increasing or decreasing the nose radius for the thick sections (0012 and 0018) has very little effect on this variation (figs. 8 and 9), while for the thin sections (fig. 7) increasing or decreasing the nose radius leads to a marked increase or decrease, respectively, of the range of lift where the profile drag is approximately constant. It may be observed that the 0006T and 0006 have about the same $C_{L\ max}$, but the rate of increase of drag with lift is greater for the thin-nosed section. This observation is in accordance with the results of reference 3, which show that the drag of the sharp-nosed airfoil (C-62) is less than the drag of the same airfoil with rounded nose (N-46) for only a small range of angle of attack. As shown by Figure 5, the minimum drag decreases with decreased nose radius, the thicker sections showing the greater effect.

Conclusions

1. The thin-nosed sections gave lower minimum drags, but also lower maximum lifts, than the normal sections.

2. The blunt-nosed sections gave higher minimum drags, but also higher maximum lifts, than the normal sections except for the thickest section (0018B) which showed a lower maximum lift.

3. The rate of increase of drag with lift is greater for the thin-nosed sections.

4. Although the slope of the lift curve varies with thickness, these tests show that for any given thickness the slope is independent of nose radius.

Langley Memorial Aeronautical Laboratory,
National Advisory Committee for Aeronautics,
Langley Field, Va., July 31, 1931.

References

1. Jacobs, Eastman N.: Tests of Six Symmetrical Airfoils in the Variable Density Wind Tunnel. N.A.C.A. Technical Note No. 385, July, 1931.

2. Jacobs, Eastman N., and Anderson, Raymond F.: Large-Scale Aerodynamic Characteristics of Airfoils as Tested in the Variable Density Wind Tunnel. N.A.C.A. Technical Report No. 352, 1930.

3. Weick, Fred E.: Tests of Four Racing-Type Airfoils in the Twenty-Foot Propeller Research Tunnel. N.A.C.A. Technical Note No. 317, September, 1929.

TABLE I

Basic Ordinates

Station in per cent chord	Ordinates in per cent chord		
	T series	Normal	B-series
0	± 0	± 0	± 0
1.25	2.08	3.16	4.74
2.5	3.14	4.36	6.15
5.0	4.76	5.92	7.65
7.5	6.01	7.00	8.47
10	7.02	7.80	8.97
15	8.49	8.91	9.57
20	9.40	9.56	9.86
30	10.00	10.00	10.00
40	9.58	9.37	9.88
50	8.52	8.82	9.31
60	7.15	7.61	8.30
70	5.65	6.11	6.79
80	4.05	4.37	4.85
90	2.28	2.41	2.58
95	1.30	1.34	1.38
100	.20	.21	.20

TABLE II

Nose Radii in Per Cent Chord

Section	T-series	Normal	B-series
0006	.10	.39	1.19
0012	.40	1.58	3.80
0018	.89	3.55	7.15

TABLE III

Airfoil: N.A.C.A. 0006T

Average Reynolds Number: 3,180,000.
Size of model: 5 X 30 inches.
Pressure, standard atmospheres: 20.8.
Test No.: 554. Variable Density Tunnel.
Date: April 8, 1931.

C_L	α_o (degrees)	C_{D_o}	$C_{m_{c/4}}$
-0.841	-11.3	0.1665	0.071
-.792	- 9.5	.1211	.040
-.577	- 6.2	.0407	-.002
-.298	- 3.1	.0099	.002
.005	0	.0069	.005
.161	1.5	.0079	.007
.311	3.0	.0123	.008
.587	6.1	.0500	.009
.793	9.5	.1355	-.041
.845	11.3	.1815	-.073
.854	13.3	.2229	-.100
.839	15.3	.2587	-.116
.830	17.4	.2923	-.126
.823	21.4	.3642	-.135
.819	27.4	.4770	-.145

TABLE IV

Airfoil: N.A.C.A. 0006

Average Reynolds Number: 3,120,000.
Size of model: 5 × 30 inches.
Pressure, standard atmospheres: 20.3.
Test No.: 555. Variable Density Tunnel.
Date: April 8, 1931.

C_L	α_o (degrees)	C_{D_o}	$C_{m_{c/4}}$
-0.847	-11.3	0.1582	0.055
-.786	- 9.5	.1324	.020
-.613	- 6.0	.0129	-.005
-.311	- 3.0	.0078	-.003
.004	0	.0070	.000
.157	1.5	.0077	.002
.315	3.0	.0084	.003
.620	6.0	.0135	.004
.794	9.5	.1195	-.025
.848	11.3	.1645	-.059
.867	13.2	.2125	-.090
.857	15.3	.2528	-.110
.835	17.3	.2877	-.125
.823	21.4	.3588	-.135
.819	27.4	.4695	-.145

TABLE V

Airfoil: N.A.C.A. 00063

Average Reynolds Number: 3,090,000.
Size of model: 5 × 30 inches.
Pressure, standard atmospheres: 20.8.
Test No.: 556. Variable Density Tunnel.
Date: April 8, 1931.

C_L	α_o (degrees)	C_{D_o}	$C_{m_{c/4}}$
-0.926	-9.1	0.0139	0.002
-.621	-6.0	.0099	-.002
-.306	-3.0	.0081	.000
-.001	0	.0076	.006
.157	1.5	.0080	.008
.312	3.0	.0085	.008
.625	6.0	.0101	.010
.934	9.0	.0143	.009
1.060	10.6	.0360	.003
1.049	12.7	.1231	-.038
.985	16.9	.2661	-.100
.870	21.2	.3506	-.125
.823	27.4	.4603	-.139

TABLE VI

Airfoil: N.A.C.A. C012T

Average Reynolds Number: 3,120,000.
Size of model: 5 X 30 inches.
Pressure, standard atmospheres: 20.5.
Test No.: 548. Variable Density Tunnel.
Date: April 3, 1931.

C_L	α_o (degrees)	C_{D_o}	$C_{m_{c/4}}$
-0.893	-9.2	0.0149	0.002
-.599	-6.1	.0112	-.001
-.298	-3.1	.0091	-.001
.007	0	.0082	.002
.159	1.5	.0085	.002
.304	3.0	.0092	.003
.609	6.1	.0114	.003
.901	9.1	.0155	.000
1.023	10.7	.0234	.000
1.030	12.7	.0812	-.020
.884	17.2	.2566	-.086
.784	21.5	.3522	-.113
.743	27.6	.4627	-.123

TABLE VII

Airfoil: N.A.C.A. 0012

Average Reynolds Number: 3,230,000.
Size of model: 5 X 30 inches.
Pressure, standard atmospheres: 20.4.
Test No.: 562. Variable Density Tunnel.
Date: April 13, 1931.

C_L	α_o (degrees)	C_{D_o}	$C_{m_{c/4}}$
-1.187	-12.2	0.0194	-0.002
-.904	-9.1	.0137	-.003
-.604	-6.1	.0108	-.005
-.299	-3.0	.0090	-.002
.003	0	.0089	-.001
.155	1.5	.0090	.001
.310	3.0	.0096	.002
.610	6.1	.0111	.008
.912	9.1	.0141	.011
1.195	12.2	.0207	.008
1.325	13.8	.0252	.003
1.413	15.2	.0337	.003
1.160	16.9	.1562	-.054
.990	20.9	.2811	-.096
.864	27.3	.4295	-.128

TABLE VIII

Airfoil: N.A.C.A. 00123

Average Reynolds Number: 3,080,000.
Size of model: 5 X 30 inches.
Pressure, standard atmospheres: 20.3.
Test No.: 550. Variable Density Tunnel.
Date: April 4, 1931.

C_L	α_o (degrees)	C_{D_o}	$C_{m_{c/4}}$
-0.922	-9.1	0.0134	-0.009
-.613	-6.0	.0110	-.006
-.308	-3.0	.0099	-.005
-.006	0	.0095	.001
.151	1.5	.0097	.000
.301	3.0	.0100	.006
.605	6.1	.0113	.010
.904	9.1	.0137	.008
1.198	12.2	.0185	.007
1.463	15.3	.0282	.006
1.502	16.0	-	-
1.165	17.7	.1598	-.043
1.018	20.8	.2468	-.080
.902	27.1	.4764	-.114

TABLE IX

Airfoil: N.A.C.A. 0018T

Average Reynolds Number: 3,150,000.
Size of model: 5 X 30 inches.
Pressure, standard atmospheres: 20.6.
Test No.: 552. Variable Density Tunnel.
Date: April 7, 1931.

C_L	α_o (degrees)	C_{D_o}	$C_{m_{c/4}}$
-1.164	-12.3	0.0240	-0.002
-.895	-9.2	.0164	-.003
-.605	-6.1	.0129	-.003
-.307	-3.0	.0108	-.002
-.006	0	.0102	.001
.147	1.5	.0106	.001
.298	3.1	.0112	.002
.597	6.1	.0130	.005
.885	9.2	.0160	.005
1.159	12.3	.0226	.003
1.281	13.9	.0283	.001
1.289	15.9	.0691	-.018
1.192	20.2	.1891	-.061
.951	27.0	.4067	-.117

TABLE X

Airfoil: N.A.C.A. 0018

Average Reynolds Number: 3,140,000.
Size of model: 5 X 30 inches.
Pressure, standard atmospheres: 20.8.
Test No.: 553. Variable Density Tunnel.
Date: April 7, 1931.

C_L	α_o (degrees)	C_{D_o}	$C_{m_{c/4}}$
-0.896	-9.2	0.0156	-0.011
-.303	-6.1	.0130	-.011
-.305	-3.0	.0113	-.006
-.006	0	.0110	-.002
.144	1.5	.0109	.002
.294	3.1	.0115	.005
.590	6.1	.0130	.009
.381	9.2	.0156	.007
1.130	12.3	.0205	.009
1.404	15.5	.0322	.012
1.429	16.5	-	-
1.309	17.8	.1107	-.018
1.251	20.0	.1735	-.036
1.023	24.7	.3022	-.082

TABLE XI

Airfoil: N.A.C.A. 00183

Average Reynolds Number: 3,180,000.
Size of model: 5 X 30 inches.
Pressure, standard atmospheres: 20.3.
Test No.: 551. Variable Density Tunnel.
Date: April 6, 1931.

C_L	α_o (degrees)	C_{D_o}	$C_{m_{c/4}}$
-0.885	-9.2	0.0174	-0.014
-.594	-6.1	.0145	-.011
-.299	-3.0	.0126	-.006
-.003	0	.0122	.001
.147	1.5	.0123	.004
.293	3.1	.0129	.007
.589	6.1	.0143	.015
.377	9.2	.0168	.019
1.146	12.4	.0227	.022
1.374	15.3	.0357	.024
1.402	16.3	.0401	.026
1.136	17.6	.1459	-.025
1.066	20.6	.2211	-.037
.820	27.4	.3711	-.090

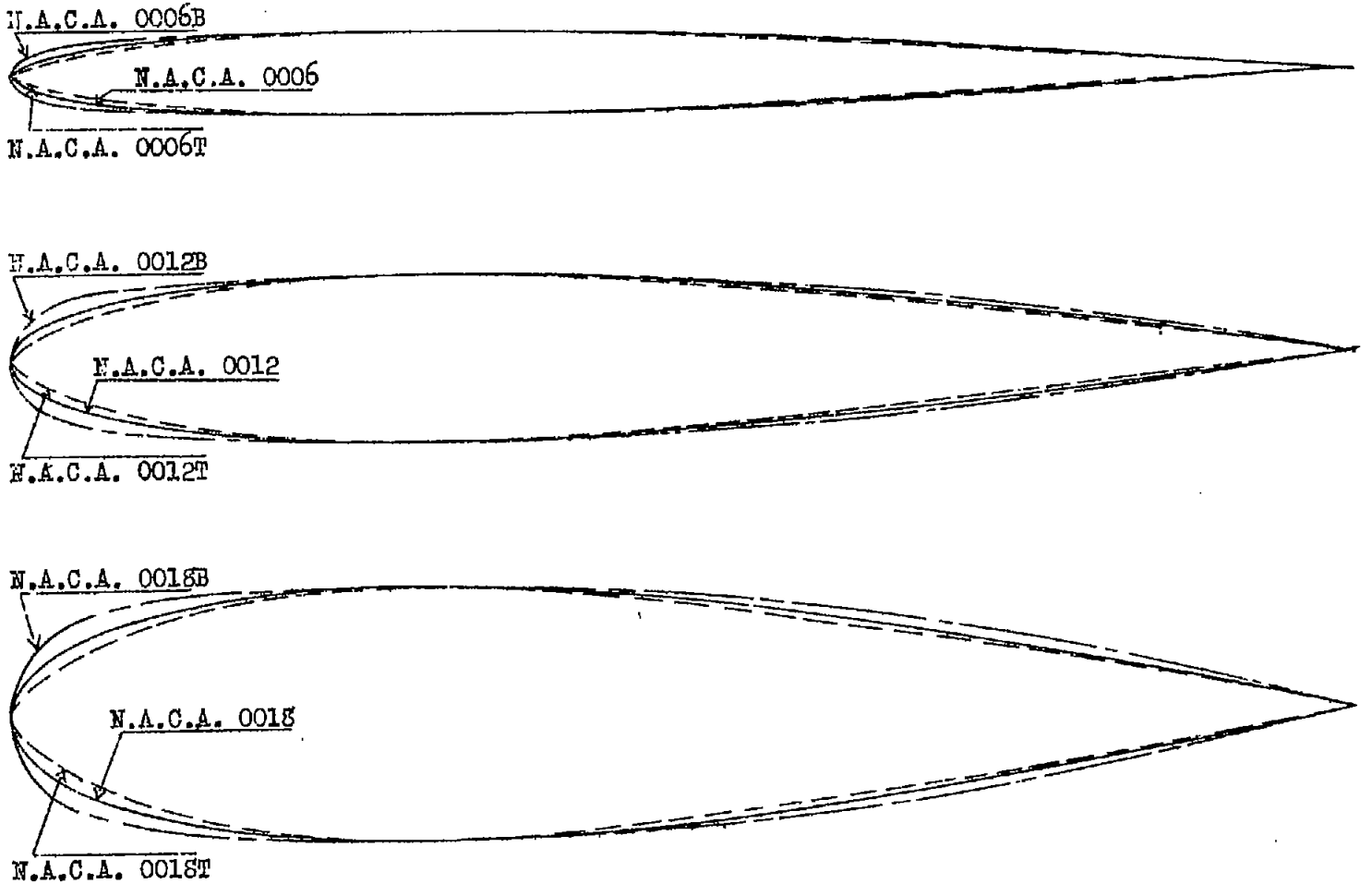

Fig.1, Profiles of N.A.C.A. symmetrical airfoils with different nose shapes.

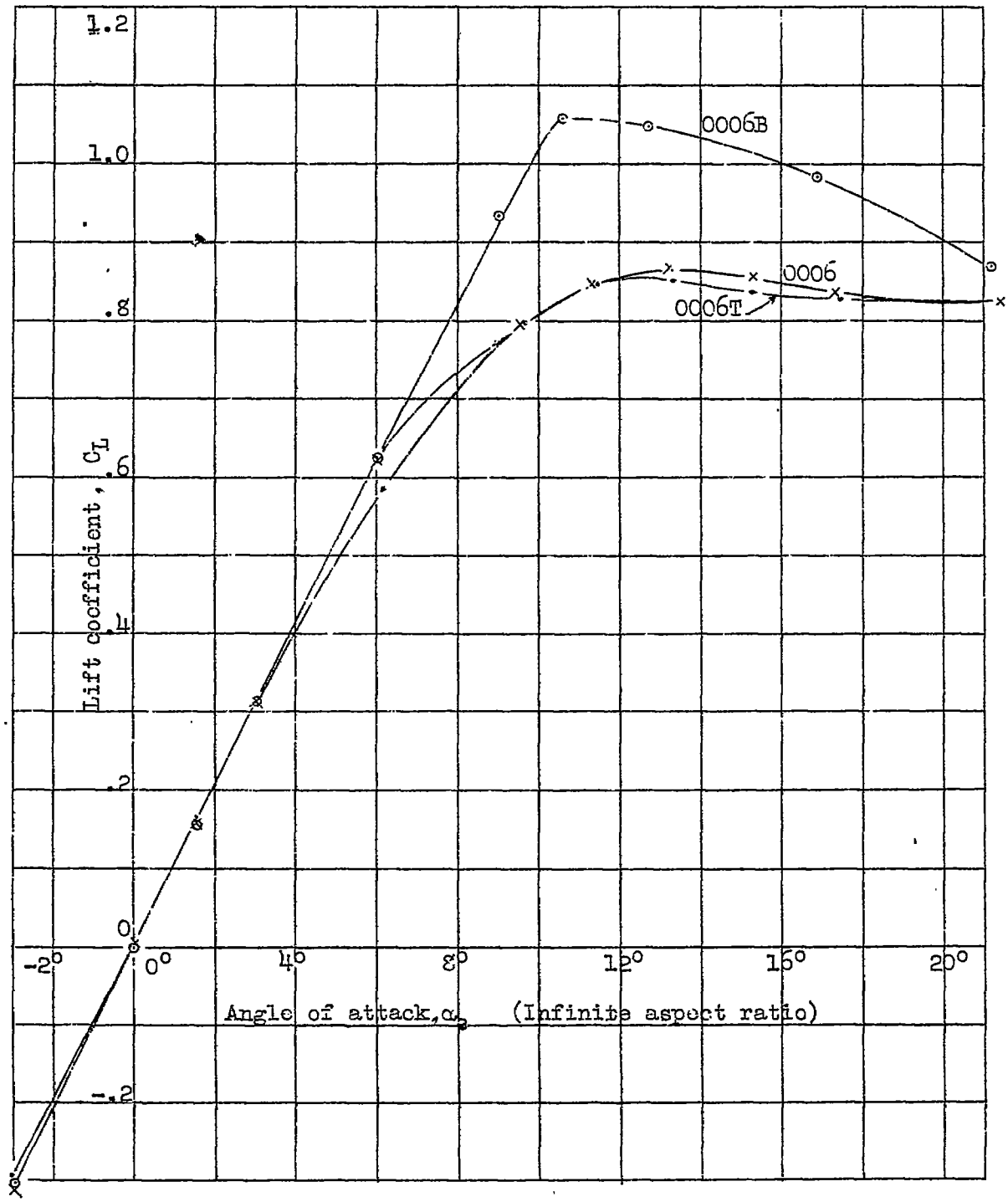

Fig.2, Lift curves for sections of maximum thickness .06

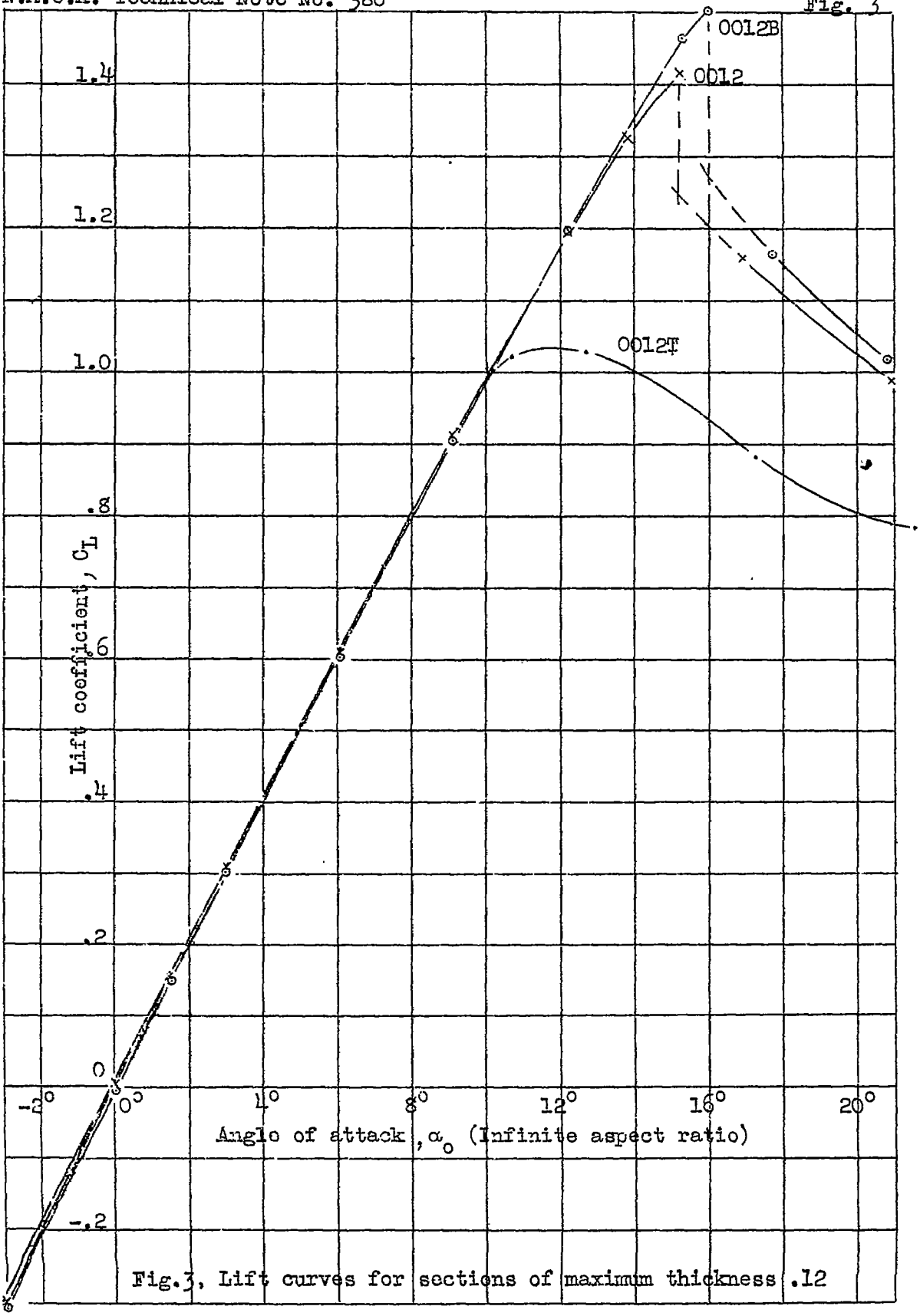

Fig.3, Lift curves for sections of maximum thickness .12

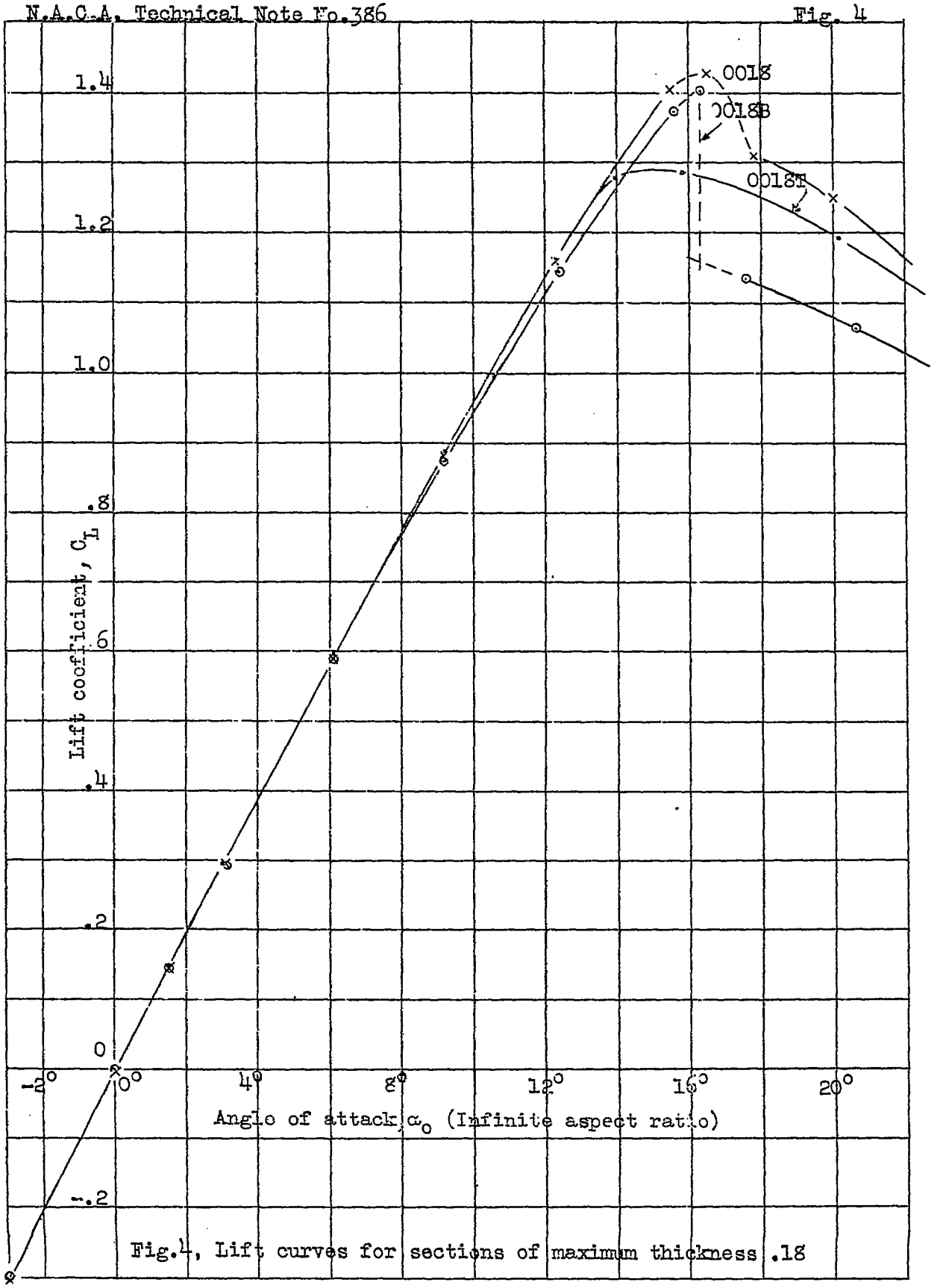

Fig.4, Lift curves for sections of maximum thickness .18

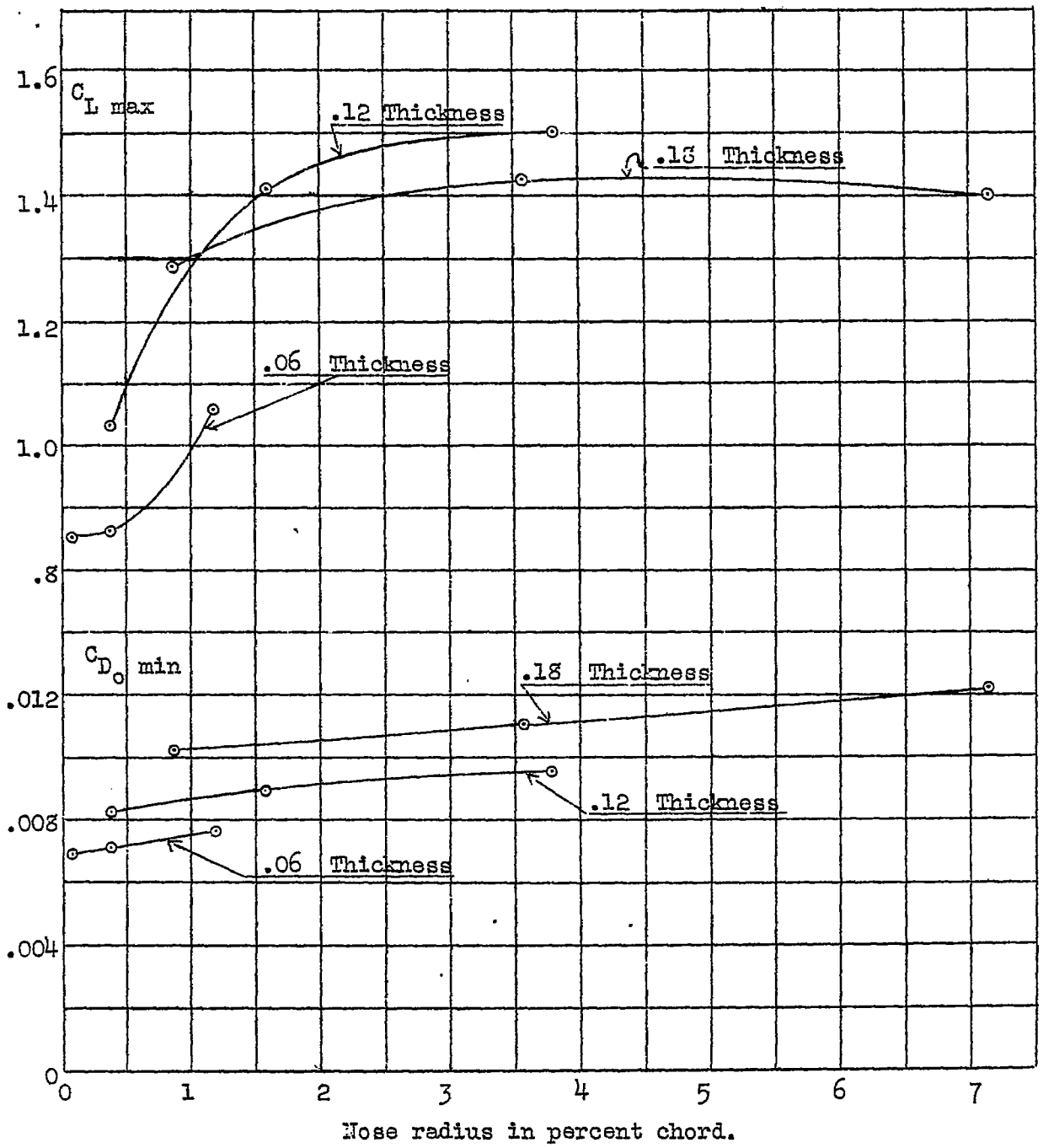

Fig.5, Variation of $C_{L\ max}$ and C_{D_o} min with nose radius.

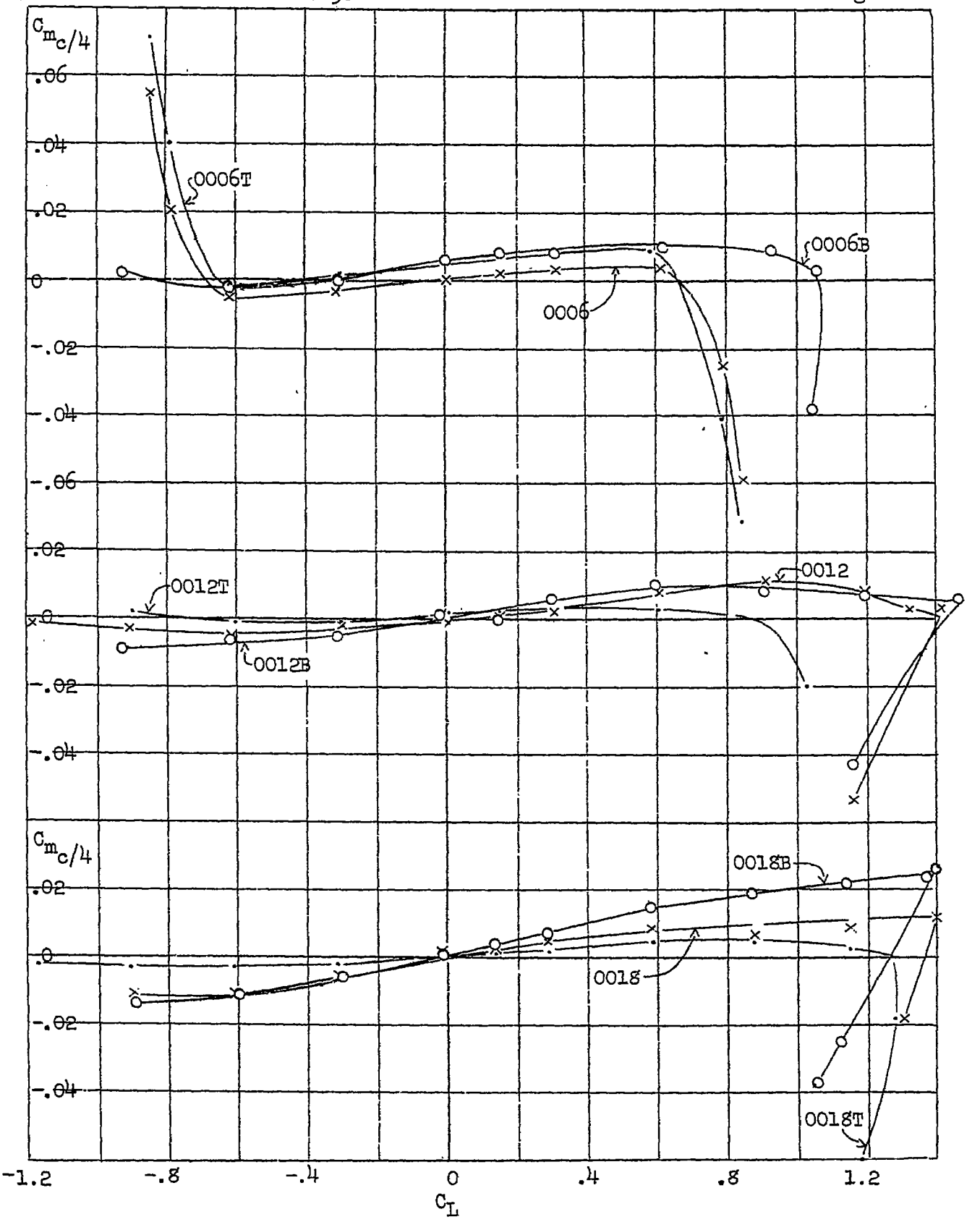

Fig.6 Variation of pitching moment coefficient with lift coefficient.

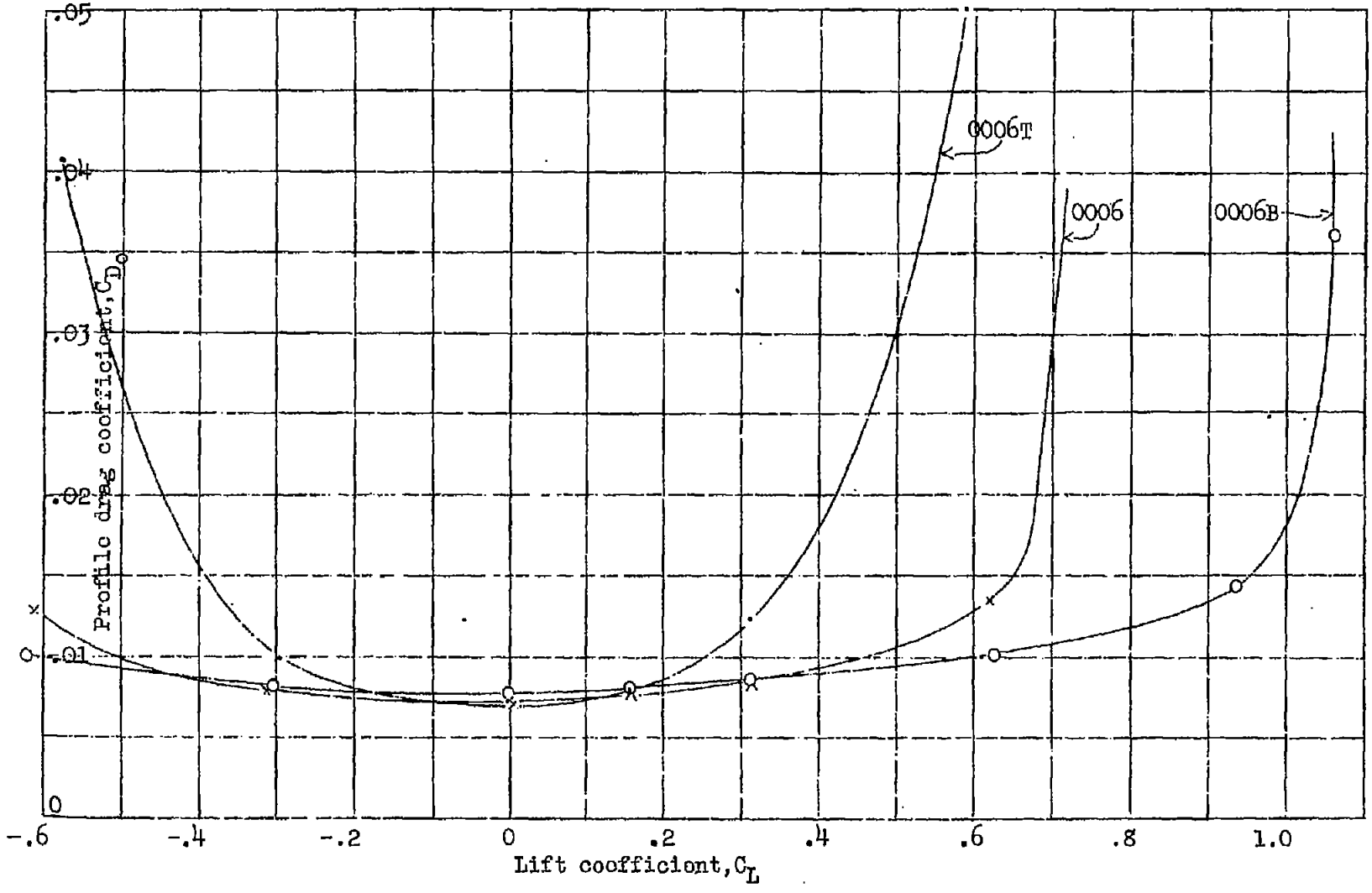

Fig.7 Profile drag curves for sections of maximum thickness .06

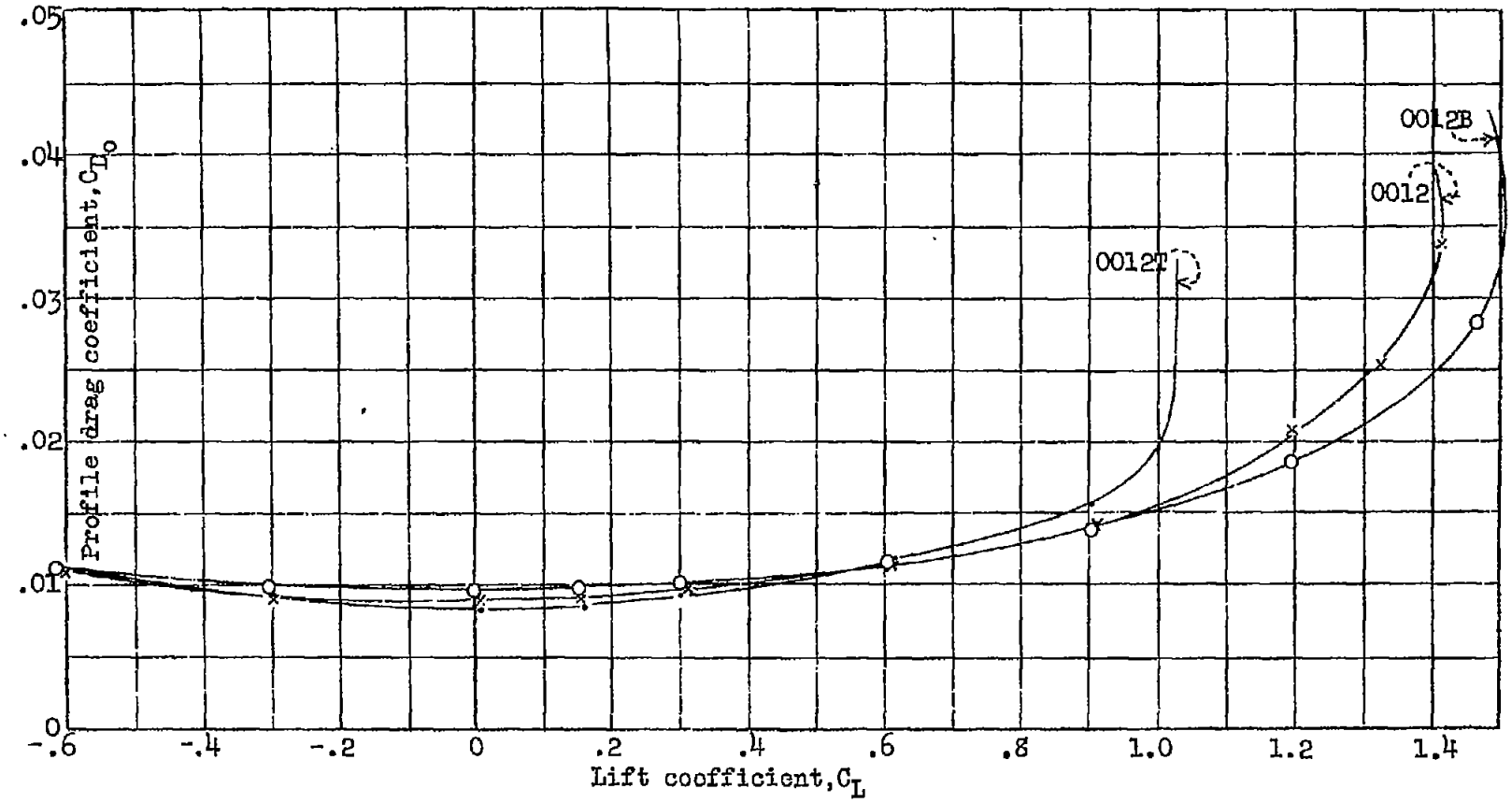

Fig.8 Profile drag curves for sections of maximum thickness .12

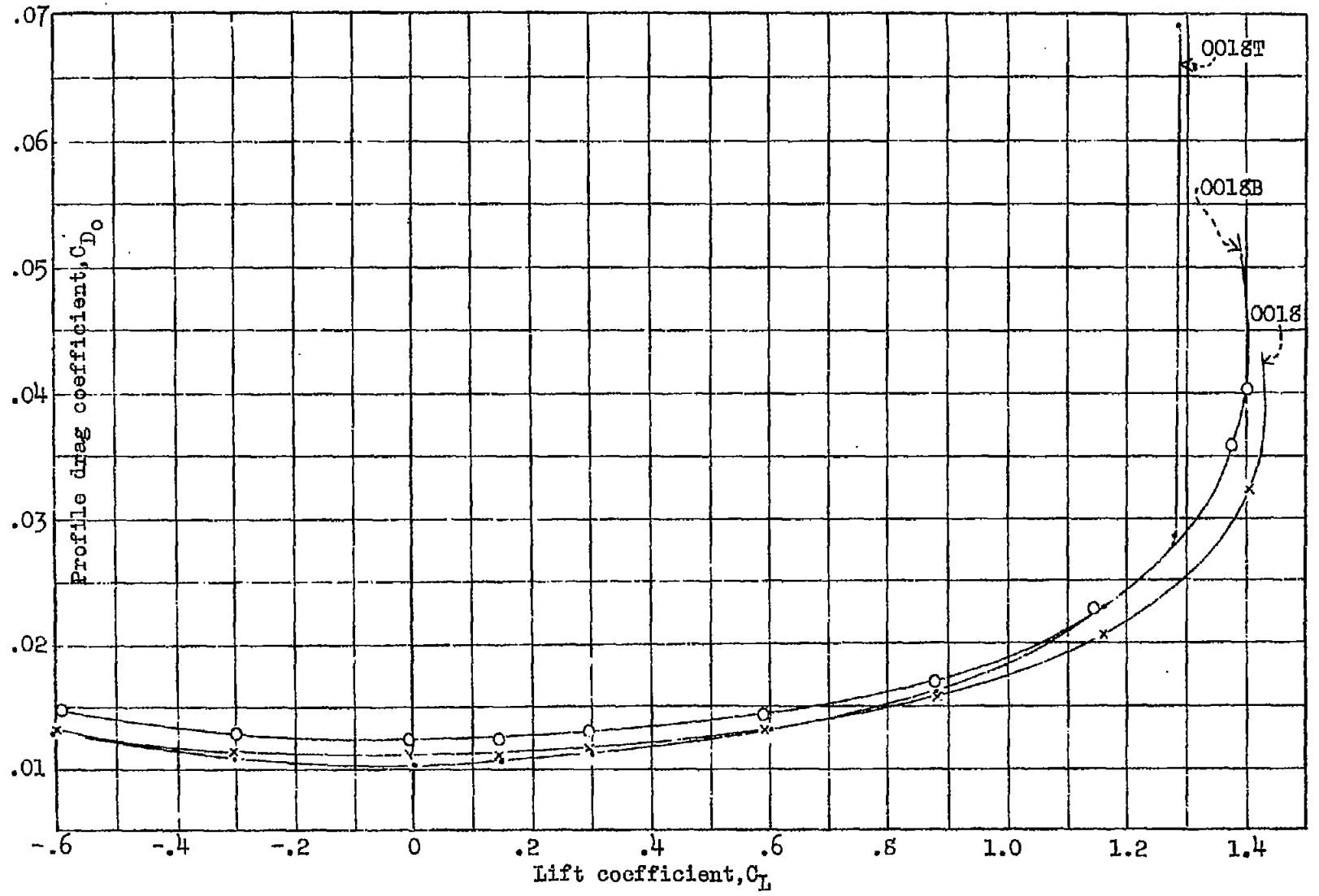

Fig.9 Profile drag curves for sections of maximum thickness .18